Electronic Supplementary Material (ESI) for Journal of Materials Chemistry B.

Supporting Information

UV-Assisted Synthesis of Long-Wavelength Si-Pyronine Fluorescent Dyes for Real-time and Dynamic Imaging of Glutathione Fluctuation in Living Cells

Hailiang Nie, Liang Qiao, Wen Yang, Bingpeng Guo, Fangyun Xin, Jing Jing* and Xiaoling Zhang*

Key Laboratory of Cluster Science of Ministry of Education, Beijing Key Laboratory of Photoelectronic/Electrophotonic Conversion Materials, School of Chemistry, Beijing Institute of Technology, 5 Zhongguancun Road, Beijing 100081, P. R. China

E-mail: zhangxl@bit.edu.cn (X. Zhang); hellojane@bit.edu.cn (J. Jing);

Contents

1. Materials and Instruments

3-bromo-*N*, *N*-dimethylaniline, *s*-BuLi, $Si(CH_3)_2Cl_2$, $Si(CH(CH_3)_2)Cl_2$, $Si(CH_3)(CH_2CH_2CF_3)Cl_2$ and $Si(C_6H_5)_2Cl_2$ were purchased from Alfa Aesar or Aldrich reagents and used as received. All solvents were used after appropriate distillation or purification. Silica gel (200–300 mesh, Qingdao Haiyang Chemical Co.) was used for column chromatography.

NMR spectra was recorded on a Bruker Avance III at 500 MHz for ^{1}HNMR. Mass spectra (MS) was acquired with a Bruker Apex IV FTMS using ESI. HPLC analysis was performed on an inertsil C18-ST (4.6 × 250 mm) column (TechMate Technology CO., LTD.) using an HPLC system composed of two pumps (LC-20AT, SHIMADZU) and a detector (SPD-M10Avp, SHIMADZU). Preparative HPLC was performed on an Inertsil C18-ST (10.0 × 250 mm) column (TechMate Technology CO., LTD.) using an HPLC system composed of two pumps (LC-6AD, SHIMADZU) and a detector (SPD-20AV, SHIMADZU). Images were captured at 30 frames/s under a Zeiss710 confocal fluorescence microscope. UV-visible spectra were obtained on a Beijing Purkinje TU-1901. Fluorescence spectroscopic studies were performed on a Hitachi F-7000. The bandwidth was 5 nm for both excitation and emission, and the photomultiplier voltage was 700 V. Absolute quantum efficiency was measured by Combined Measurement System for Infrared Fluorescence (Nanolog^R FluoroLog-3-2-iHR320).

2. Cell culture and imaging

HeLa cells were cultured in Dulbecco's modified Eagle medium (DMEM) supplemented with 10% (v/v) fetal bovine serum, penicillin (100 units/mL) and streptomycin (100 μg/mL) in a humidified incubator containing 5% CO_2 gas. Before use, the adherent cells were washed three times with FBS-free DMEM. For imaging, the cells were incubated with SiP-Pr (final concertation: 1μM) in FBS-free DMEM at 37 ℃, while being observed under a Zeiss710 confocal fluorescence microscope with excitation wavelength fixed at 633 nm and fluorescence wavelengths at 638-758 nm.

3. Synthesis of SiPs

4, 4'-methylenebis(3-bromo-N, N-dimethylaniline)

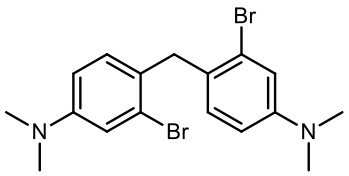

The chemical structure of 4, 4'-methylenebis(3-bromo-N, N-dimethylaniline)

To 3-bromo-*N*, *N*-dimethylaniline (5.00 g, 25.00 mmol) in AcOH (50 mL) was added 37% formaldehyde solution (5 ml), and the mixture was stirred for 30 min at 60 °C. After cooling, saturated $NaHCO_3$ aqueous solution was added carefully until no gas evolved. The aqueous solution was extracted with ethyl acetate, and the organic phase was washed with brine, dried over $MgSO_4$, then filtered and evaporated. The residue was purified by silica gel column chromatography (*n*-hexane/EtOAc = 5/1) to obtain 4, 4'-methylenebis(3-bromo-*N*,*N*-dimethylaniline) as a white solid (3.10 g, 60%).
^{1}H NMR (400 MHz, Chloroform-*d*) δ 6.96 (s, 2H), 6.86 (d, *J* = 8.5 Hz, 2H), 6.61 (d, *J* = 7.3 Hz, 2H), 4.01 (s, 2H), 2.92 (s, 12H).

SiP-Me

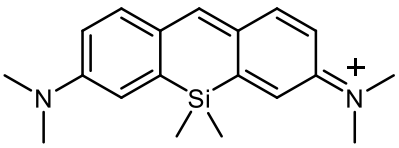

The chemical structure of SiP-Me

To a dried flash flushed with argon, 4, 4’-methylenebis(3-bromo-*N*,*N*-dimethylaniline) (0.103 g, 0.25 mmol) dissolved in dry THF (5.0 ml) was added. The solution was cooled to – 78 °C, 1.3 M *s*-BuLi (0.50 mL, 0.575 mmol) was added, and the mixture was stirred for 60 min. At the same temperature, $Si(CH_3)_2Cl_2$ (0.042 g, 0.325 mmol) dissolved in anhydrous THF (2 mL) was added to the reaction mixture, and the mixture was warmed to room temperature, then stirred for 4 h. The reaction was quenched by addition of 2 N HCl aqueous solution and stirring was continued at r.t.

for 10 min. Saturated $NaHCO_3$ aqueous solution was added, and the whole was extracted with CH_2Cl_2. The organic layer was dried over $MgSO_4$ and evaporated. The residue was dissolved in CH_2Cl_2 (50 mL), and then was irradiated under 254 nm ultraviolet light. The mixture was stirred for 4 h, and the solvent was evaporated again. The residue was purified by preparative reverse-phase HPLC with a linear gradient [C18-ST: starting eluent 20% CH_3CN/0.1% TFA aq; final eluent 80% CH_3CN/0.1% TFA aq.; gradient duration 20 min; flow rate = 4 mL/min]. Fractions containing the product were combined and freeze-dried to afford SiP-Me as a deep blue solid **(**TFA salt, 0.031g, 29 % yield).

^{1}H NMR (400 MHz, Methanol-d4) δ 7.87 (s, 1H), 7.71 (d, *J* = 9.2 Hz, 2H), 7.33 (d, *J* = 2.7 Hz, 2H), 6.98 (dd, *J* = 9.2, 2.7 Hz, 2H), 3.38 (s, 12H), 0.55 (s, 6H).

HRMS (ESI) m/z Found 309.1783 M^+, calculated 309.1782 for $C_{19}H_{25}SiN_2$ (-0.37 ppm)

$C_{19}H_{25}N_2Si^+Cl^-$ elemental analysis (%): found C 66.29, H 7.45, N 8.07, Si+Cl 18.19; calculated C 66.16, H 7.31, N 8.12, Si+Cl 18.41.

HPLC chromatogram after purification:

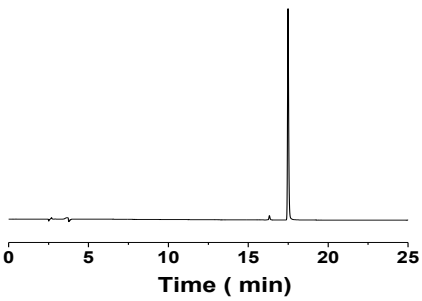

HPLC chromatogram of SiP-Me

SiP-F

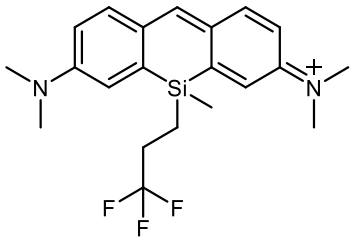

The chemical structure of SiP-F

To a dried flash flushed with argon, 4, 4'-methylenebis(3-bromo-*N*,*N*-dimethylaniline) (0.103 g, 0.25 mmol) dissolved in dry THF (5.0 ml) was added. The solution was cooled to – 78 °C, 1.3 M *s*-BuLi (0.50 mL, 0.575 mmol) was added, and the mixture was stirred for 60 min. At the same temperature, $Si(CH_3)(CH_2CH_2CF_3)Cl_2$ (0.068 g, 0.325 mmol) dissolved in anhydrous THF (2 mL) was added to the reaction mixture, and the mixture was warmed to room temperature, then stirred for 4 h. The reaction was quenched by addition of 2 N HCl aqueous solution and stirring was continued at r.t. for 10 min. Saturated $NaHCO_3$ aqueous solution was added, and the whole was extracted with CH_2Cl_2. The organic layer was dried over $MgSO_4$ and evaporated. The residue was dissolved in CH_2Cl_2 (50 mL), and then was irradiated under ultraviolet light (254 nm). The mixture was stirred for 3 h, and the solvent was evaporated again. The residue was purified by preparative reverse-phase HPLC with a linear gradient [C18-ST: starting eluent 20% CH_3CN/0.1% TFA aq; final eluent 80% CH_3CN/0.1% TFA aq.; gradient duration 20 min; flow rate = 4 mL/min]. Fractions containing the product were combined and freeze-dried to afford SiP-F as a deep blue solid **(**TFA salt, 0.033g, 26 % yield).

^{1}H NMR (500 MHz, Methanol-d4) δ 7.68 (s, 1H), 7.53 (d, *J* = 9.2 Hz, 2H), 7.15 (d, *J* = 2.4 Hz, 2H), 6.80 (dd, *J* = 9.2, 2.7 Hz, 2H), 3.17 (s, 12H), 1.73 (s, 2H), 1.09 – 1.03 (m, 2H), 0.44 (s, 3H).

HRMS (ESI) m/z Found 391.1815 M^+, calculated 391.1812 for $C_{21}H_{26}F_3SiN_2$ (-0.77 ppm)

$C_{21}H_{26}F_3N_2Si^+Cl^-$ elemental analysis (%): found C 59.45, H 6.53, N 6.15, F+Si+Cl 27.87; calculated C 59.07, H 6.14, N 6.56, F+Si+Cl 28.23.

HPLC chromatogram after purification:

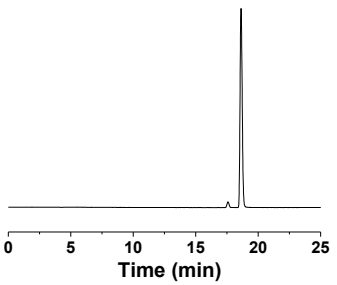

HPLC chromatogram of SiP-F

SiP-Pr

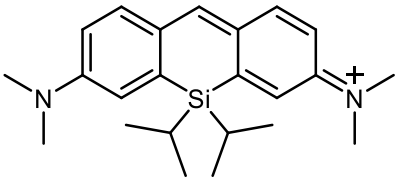

The chemical structure of SiP-Pr

To a dried flash flushed with argon, 4, 4'-methylenebis(3-bromo-*N*,*N*-dimethylaniline) (0.103 g, 0.25 mmol) dissolved in dry THF (5.0 ml) was added. The solution was cooled to – 78 °C, 1.3 M *s*-BuLi (0.50 mL, 0.575 mmol) was added, and the mixture was stirred for 60 min. At the same temperature, $Si(CH(CH_3)_2)Cl_2$ (0.061 g, 0.325 mmol) dissolved in anhydrous THF (2 mL) was added to the reaction mixture, and the mixture was warmed to room temperature, then stirred for 4 h. The reaction was quenched by addition of 2 N HCl aqueous solution and stirring was continued at r.t. for 10 min. Saturated $NaHCO_3$ aqueous solution was added, and the whole was extracted with CH_2Cl_2. The organic layer was dried over $MgSO_4$ and evaporated. The residue was dissolved in CH_2Cl_2 (50 mL), and then was irradiated under ultraviolet light (254 nm). The mixture was stirred for 3 h, and the solvent was evaporated again. The residue was purified by preparative reverse-phase HPLC with a linear gradient [C18-ST: starting eluent 20% CH_3CN/0.1% TFA aq; final eluent 80% CH_3CN/0.1% TFA aq.; gradient duration 20 min; flow rate = 4 mL/min]. Fractions containing the product were combined and freeze-dried to afford SiP-F as a deep blue solid **(**TFA salt, 0.037g, 31 % yield).

^{1}H NMR (500 MHz, Methanol-d4) δ 7.93 (s, 1H), 7.77 (d, *J* = 9.2 Hz, 2H), 7.22 (d, *J* = 2.1 Hz, 2H), 7.04 (dd, *J* = 9.2, 2.7 Hz, 2H), 3.39 (s, 12H), 1.56 (dq, *J* = 14.7, 7.4 Hz, 2H), 1.05 (d, *J* = 7.4 Hz, 12H).

HRMS (ESI) m/z Found 365.2411M^+, calculated 365.2408 for $C_{23}H_{33}N_2Si$ (-0.79 ppm)

$C_{23}H_{33}N_2Si^+Cl^-$ elemental analysis (%): found C 69.31, H 8.72, N 6.59, Si+Cl 15.38; calculated C 68.88, H 8.29, N 6.98, Si+Cl 15.85.

HPLC chromatogram after purification:

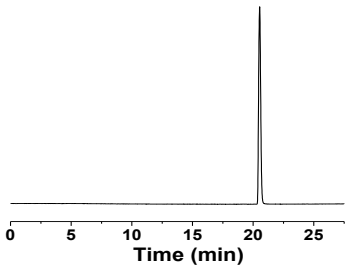

HPLC chromatogram of SiP-Pr

SiP-Ph

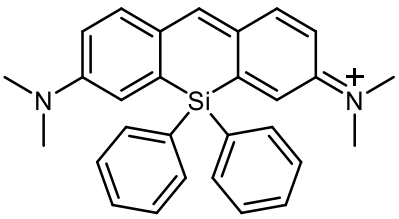

The chemical structure of SiP-Ph

To a dried flash flushed with argon, 4, 4'-methylenebis(3-bromo-*N*,*N*-dimethylaniline) (0.103 g, 0.25 mmol) dissolved in dry THF (5.0 ml) was added. The solution was cooled to – 78 °C, 1.3 M *s*-BuLi (0.50 mL, 0.575 mmol) was added, and the mixture was stirred for 60 min. At the same temperature, $Si(C_6H_5)_2Cl_2$ (0.069 g, 0.325 mmol) dissolved in anhydrous THF (2 mL) was added to the reaction mixture, and the mixture was warmed to room temperature, then stirred for 4 h. The reaction was quenched by addition of 2 N HCl aqueous solution and stirring was continued at r.t. for 10 min. Saturated $NaHCO_3$ aqueous solution was added, and the whole was extracted with CH_2Cl_2. The organic layer was dried over $MgSO_4$ and evaporated. The residue was dissolved in CH_2Cl_2 (50 mL), and then was irradiated under ultraviolet light (254 nm). The mixture was stirred for 4 h, and the solvent was evaporated again. The residue was purified by preparative reverse-phase HPLC with a linear gradient [C18-ST: starting eluent 20% CH_3CN/0.1% TFA aq; final eluent 80% CH_3CN/0.1% TFA aq.; gradient duration 20 min; flow rate = 4 mL/min]. Fractions containing the product were combined and freeze-dried to afford SiP-F as a deep blue solid **(**TFA salt, 0.048g, 35 % yield).

HRMS (ESI) m/z Found 433.2095M^+, calculated 433.2095 for $C_{29}H_{29}N_2Si$ (0 ppm)

$C_{29}H_{29}N_2Si^+Cl^-$ elemental analysis: found C 74.27, H 6.62, N 5.43, Si+Cl 13.68; calculated (%) C 74.25, H 6.23, N 5.97, Si+Cl 13.55.

HPLC chromatogram after purification:

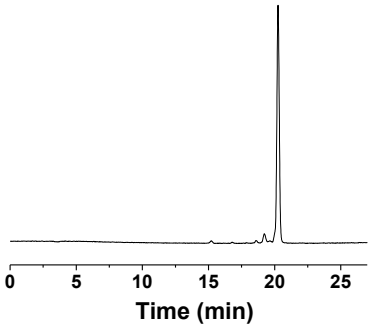

HPLC chromatogram of SiP-Ph

4. pH-dependent absorption and fluorescence spectral of SiPs and OP

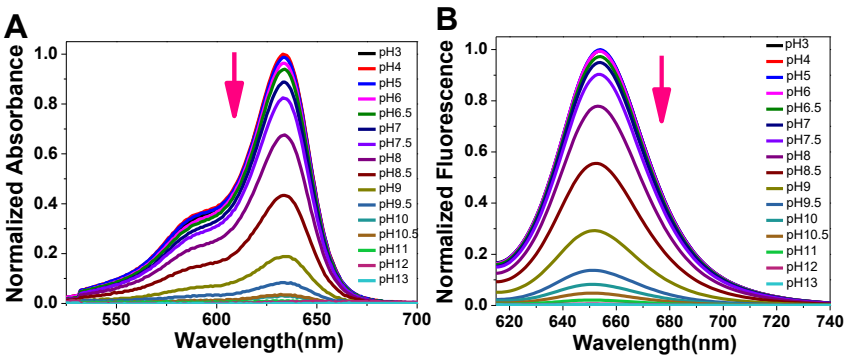

Figure S1. Normalized absorption **(A)** and fluorescence **(B)** spectra of SiP-Me in PBS solution (50 mM, pH=3, 4, 5, 6, 6.5, 7, 7.5, 8, 8.5, 9, 9.5, 10, 10.5, 11, 12, 13). The excitation wavelength was 605 nm.

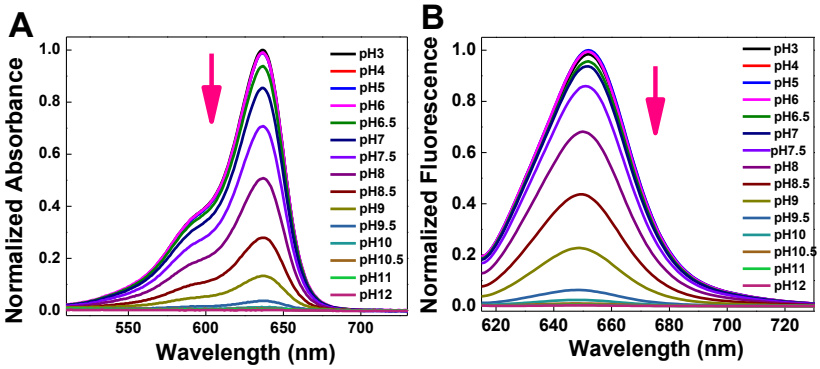

Figure S2. Normalized absorption **(A)** and fluorescence **(B)** spectra of SiP-F in PBS

solution (50 mM, pH= 3, 4, 5, 6, 6.5, 7, 7.5, 8, 8.5, 9, 9.5, 10, 10.5, 11, 12). The excitation wavelength was 605 nm.

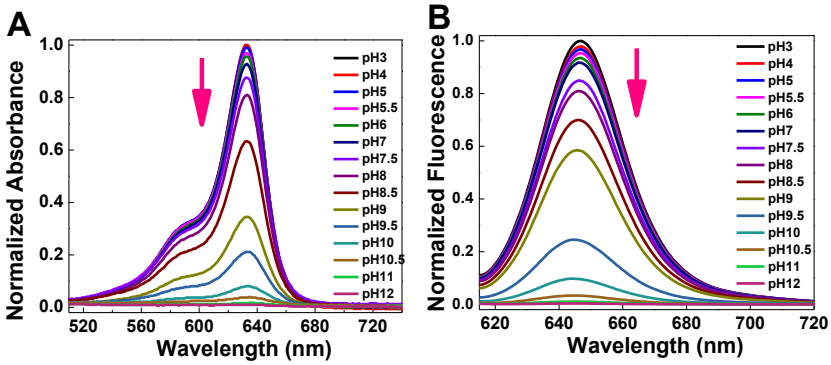

Figure S3. Normalized absorption **(A)** and fluorescence **(B)** spectra of SiP-Pr in PBS solution (50 mM, pH= 3, 4, 5, 5.5, 6, 7, 7.5, 8, 8.5, 9, 9.5, 10, 10.5, 11, 12). The excitation wavelength was 605 nm.

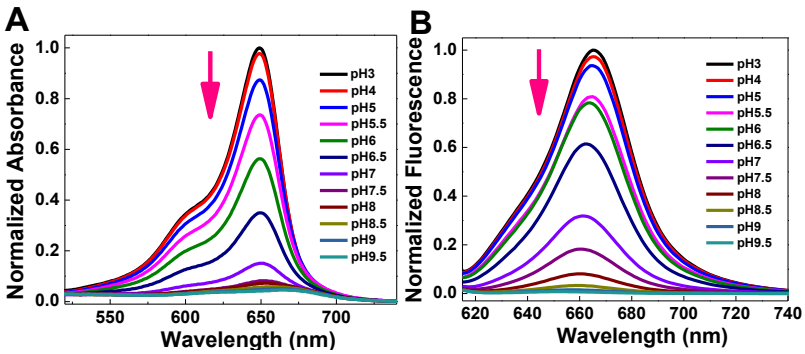

Figure S4. Normalized absorption **(A)** and fluorescence **(B)** spectra of SiP-Ph in PBS solution (50 mM, pH= 3, 4, 5, 5.5, 6, 6.5, 7, 7.5, 8, 8.5, 9, 9.5). The excitation wavelength was 605 nm.

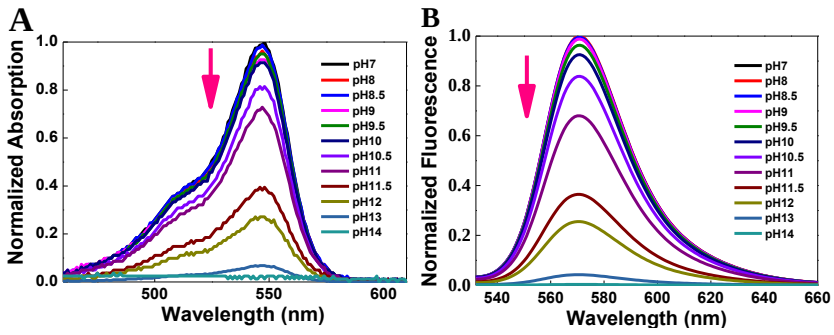

Figure S5. Normalized absorption **(A)** and fluorescence **(B)** spectra of OP in PBS

solution (50 mM, pH= 7, 8, 8.5, 9, 9.5, 10, 10.5, 11, 11.5, 12, 13, 14). The excitation wavelength was 522 nm.

5. The responsive mechanism of SiPs toward thiols

NMR spectroscopy was used to explore the reaction mechanism. Mercaptoacetic acid (MA) with the advantages of structural simplicity and excellent solubility in CD_3OD was used as the representative thiol. In CD_3OD, SiP-Me existed in a cationic form and its proton resonance peaks in the aromatic region were well assigned as listed in the following figure. After addition of MA into the CD_3OD solution of SiP-Me, proton **a** (δ 7.87) was greatly shifted to high field (δ 5.40), indicating that the central carbon was attacked by the sulfhydryl group of MA. The chemical shifts of the other aromatic protons exhibited small changes and were still in the chemical shift range of aromatic hydrogen, indicating that the aromatic ring was not disrupted. Then, the resulting solution was diluted with PBS solution (50 mM), an excess amount of NEM was added, and the mixture was separated by HPLC. Proton-NMR showed that all the proton signals were shifted back to their original positions, showing excellent reversibility.

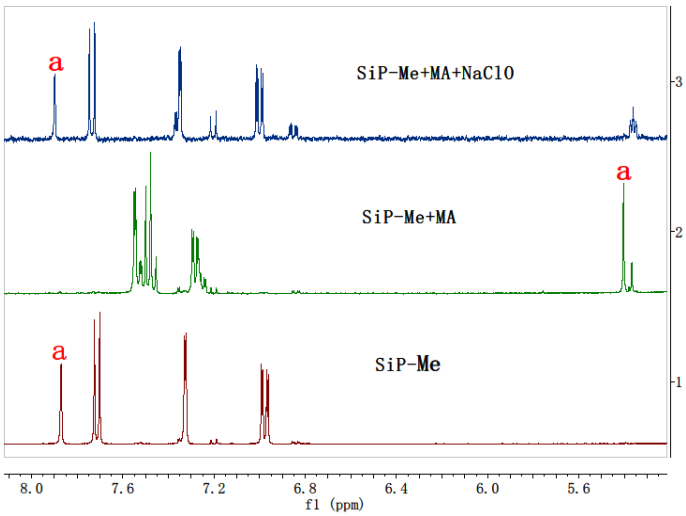

Figure S6. ^{1}H-NMR spectra of SiP-Me after sequential reaction with Mercaptoacetic acid (MA) and NEM. Non-aromatic and solvent ^{1}H NMR peaks were omitted for clarity.

6. The effect of GSH in fluorescence intensity of SiPs and OP

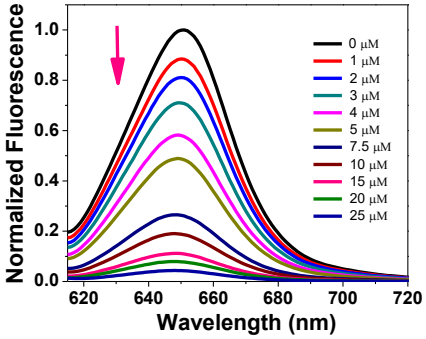

Figure S7. Normalized fluorescence intensity of SiP-F (5 μM) respond to various concentrations (0~25 μM) of GSH in PBS solution (50 mM, pH=7.4). The excitation wavelength was 605 nm.

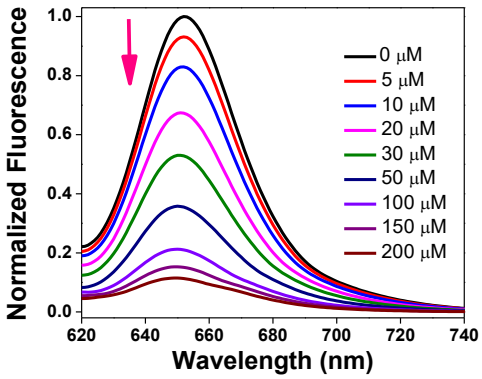

Figure S8. Normalized fluorescence intensity of SiP-Pr (5 μM) respond to various concentrations (0~200 μM) of GSH in PBS solution (50 mM, pH=7.4). The excitation wavelength was 605 nm.

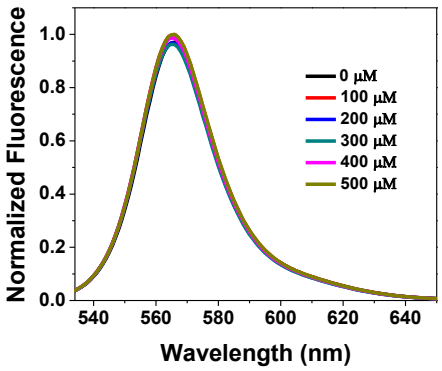

Figure S9. Normalized fluorescence intensity of OP (5 μM) respond to various concentration (0~500 μM) of GSH in PBS solution (50 mM, pH= 7.4). The excitation wavelength was 522 nm.

7. Linear relationship between the fluorescence intensity of SiPs and GSH concentration

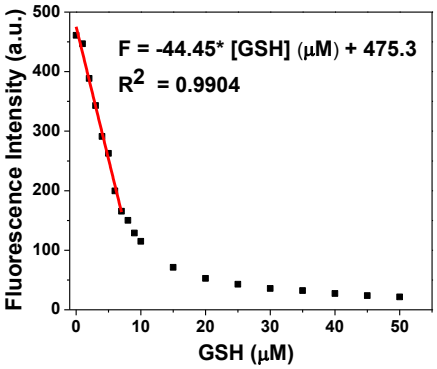

Figure S10. The linear relationship between the fluorescence intensity of SiP-Me (5 μM) and GSH concentration of up to 7 μM. The experiments were performed in PBS solution (50 mM, pH=7.4). The fluorescence intensity was measured at 650 nm, with excitation at 605 nm.

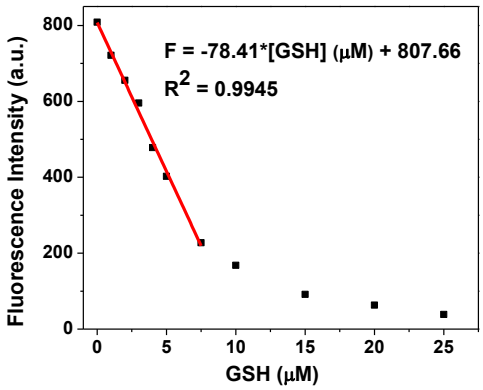

Figure S11. The linear relationship between the fluorescence intensity of SiP-F (5 μM) and GSH concentration of up to 7.5 μM. The experiments were performed in PBS solution (50 mM, pH=7.4). The fluorescence intensity was measured at 650 nm, with excitation at 605 nm.

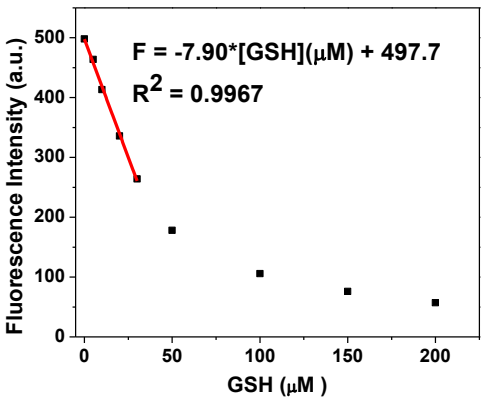

Figure S12. The linear relationship between the fluorescence intensity of SiP-Pr (5 μM) and GSH concentration of up to 30 μM. The experiments were performed in PBS solution (50 mM, pH=7.4). The fluorescence was measured at 650 nm, with excitation at 605 nm.

8. Determination of the detection limit for GSH sensing

The detection limit was calculated based on the fluorescence titration. In the absence of GSH, the fluorescence emission of SiPs was measured by ten times and the standard deviation of blank measurement was achieved. To gain the slope, the fluorescence intensity at 650 nm was plotted versus the GSH concentration. The detection limit was calculated with the following equation:

$$\text{Detection limit} = 3\sigma/k$$

Where σ is the standard deviation of blank measurement, k is the slope of the fluorescence intensity versus the GSH concentration.

9. The selective response of SiP-Me toward GSH in the presence of various ions.

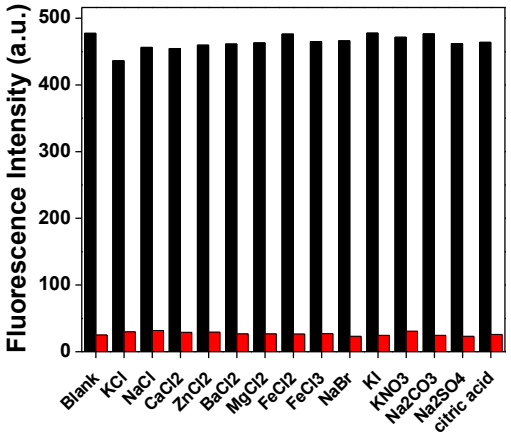

Figure S13. The fluorescence intensity of SiP-Me (5 μM) selectively respond to GSH (50 μM) in the presence of various cations and anions (1 mM for each ion, 100 μM for citric acid) in PBS solution (50 mM, pH=7.4). The blank bars show the fluorescence intensity in only presence of various ions, and the red bars show the fluorescence changes after addition of GSH. The fluorescence was measured at 650 nm, with excitation at 605 nm.

10. Response speed of SiP-Me toward various biological reductants

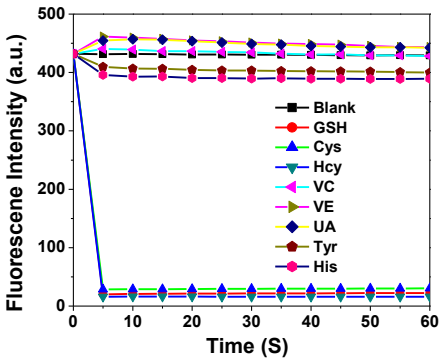

Figure S14. The fluorescence time scan of the maximum fluorescence intensity in the presence of various reductants including glutathione (GSH), cysteine (Cys), homocysteine (Hcy), vitamin C (VC), vitamin E (VE), uric acid (UC), tyrosine (Tyr) and histidine (His). The fluorescence intensity was measured at 650 nm, with excitation at 605 nm.

11. NEM effect on the reversible reaction between SiP-Me and GSH

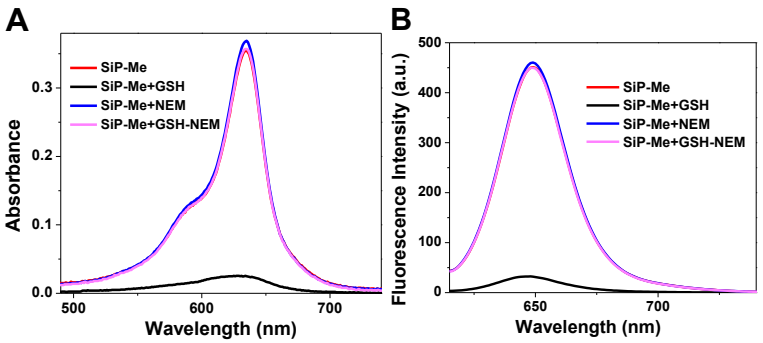

Figure S15. (A) Absorption spectra and (B) emission spectra of SiP-Me (5 μM) in the presence of GSH (50 μM), NEM (50 μM) and GSH-NEM (generated form the reaction between 50 μM GSH and 50 μM NEM in PBS solution for 1 h at r.t.). All experiments were performed in PBS solution (50 mM, pH=7.4). The emission spectra was excited at 605 nm.

12. SiP-Me-GSH time-resolved fluorescence intensity curve under NEM addition

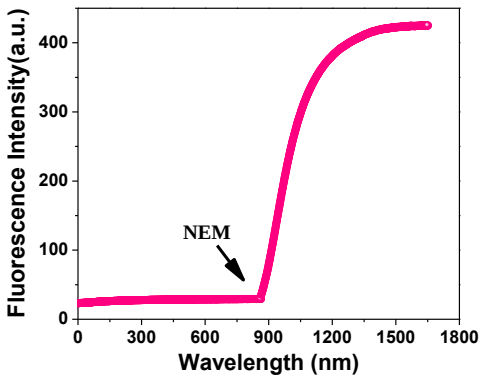

Figure S16. Changes in the maximum fluorescence intensity of SiP-Me-GSH (generated from 5 μM SiP +50 μM GSH) before and after addition of NEM (50 μM) in PBS solution (50 mM, pH=7.4). The fluorescence was measured at 650 nm, with excitation at 605 nm.

13. pH interference on GSH fluorescence detection

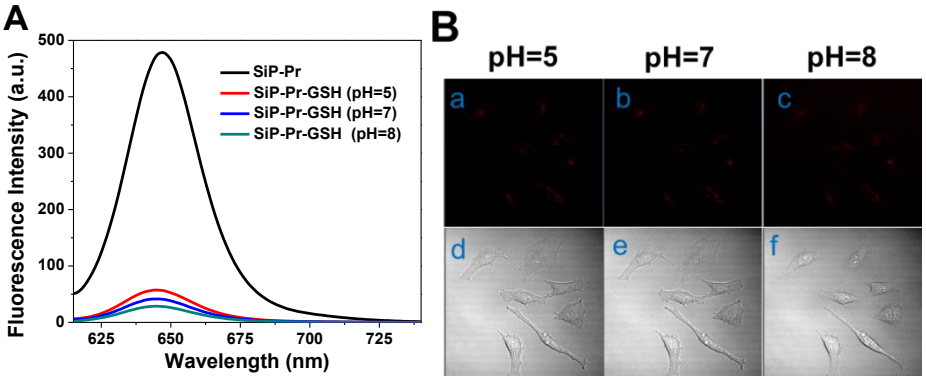

Figure S17. pH interference on GSH fluorescence detection in vitro and living cells. (A) Comparison of the SiP-Pr (5 μM) – GSH (200 μM) reaction in different pH PBS solution for 30 min at r.m.. (B) Confocal microscopic images of intracellular GSH in HeLa cells treated with different pH buffers. The cells were pre-cultured with 1 μM SiP-Pr for 30 min and then sequentially incubated in PBS Buffer of pH=5, pH=7 and pH=8 containing nigericin (1μg/mL), which could homogenize the intracellular pH to that of the incubating buffers. Incubation was performed at 37 ℃ in a humidified atmosphere containing 5% CO_2 in living cell workstation. The fluorescence was measured at 638~758 nm, with excitation at 633 nm.

14. Cytotoxicity assays of SiP-Pr

HeLa cells were cultured in culture media (DMEM) in an atmosphere of 5% CO_2 and 95% air at 37 °C. The cells were seeded into 96-well plates at a density of 5×10^3 cells per well in culture media. Then 0, 1, 2.5 and 5 μM (final concentration) SiP-Pr was added respectively. Next, the cells were incubated at 37 °C in an atmosphere of 5% CO_2 and 95% air for 24 h. Finally, 20 μL 3-(4, 5-dimethylthiazol-2-yl)-2, 5-diphenyltetrazolium bromide (MTT, 5 mg/mL) was added, and the cells were cultured for another 4 h.

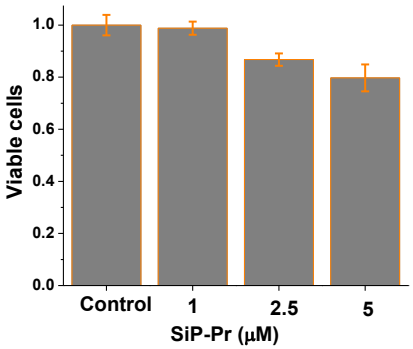

Figure S18. Cytotoxicity assays of SiP-Pr at different concentrations for HeLa cells.

15. The characterization data of SiPs

Characterization of SiP-Me

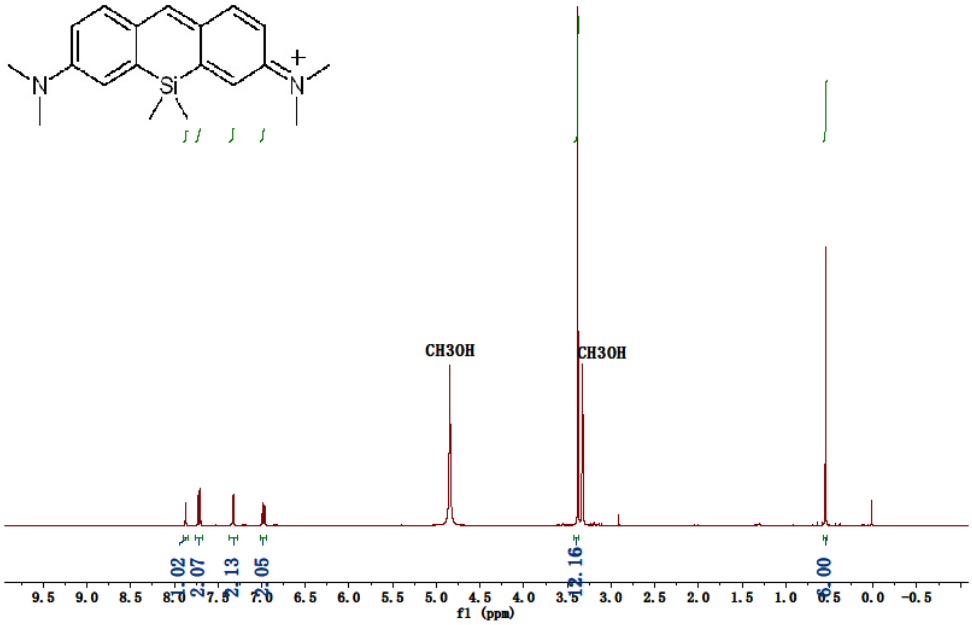

Figure S19. ^{1}H-NMR of SiP-Me

HIGH RESLUTION MASS SPECTROMETRY REPORT

Sample No.	Formula (M)	Ion Formula	Measured m/z	Calc m/z	Diff (ppm)
SiP-Me	C19 H25 N2 Si	C19 H25 N2 Si	309.1783	309.1782	-0.37

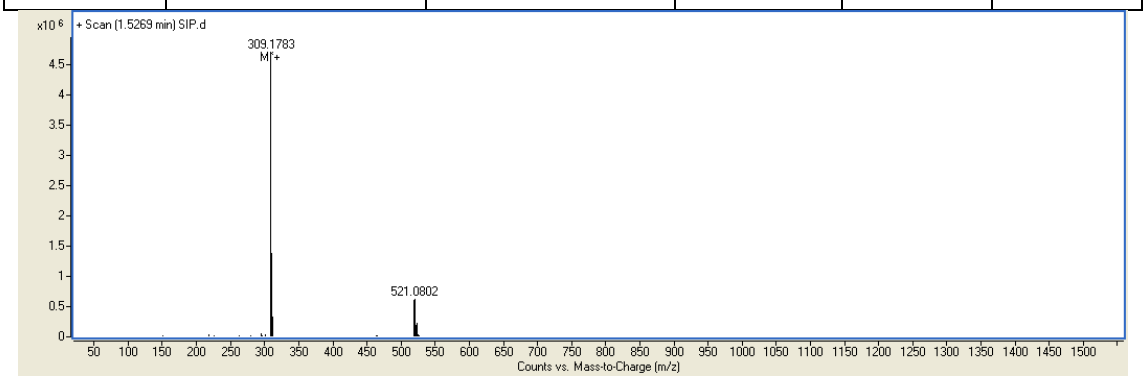

Figure S20. HRMS of SiP-Me

Characterization of SiP-F

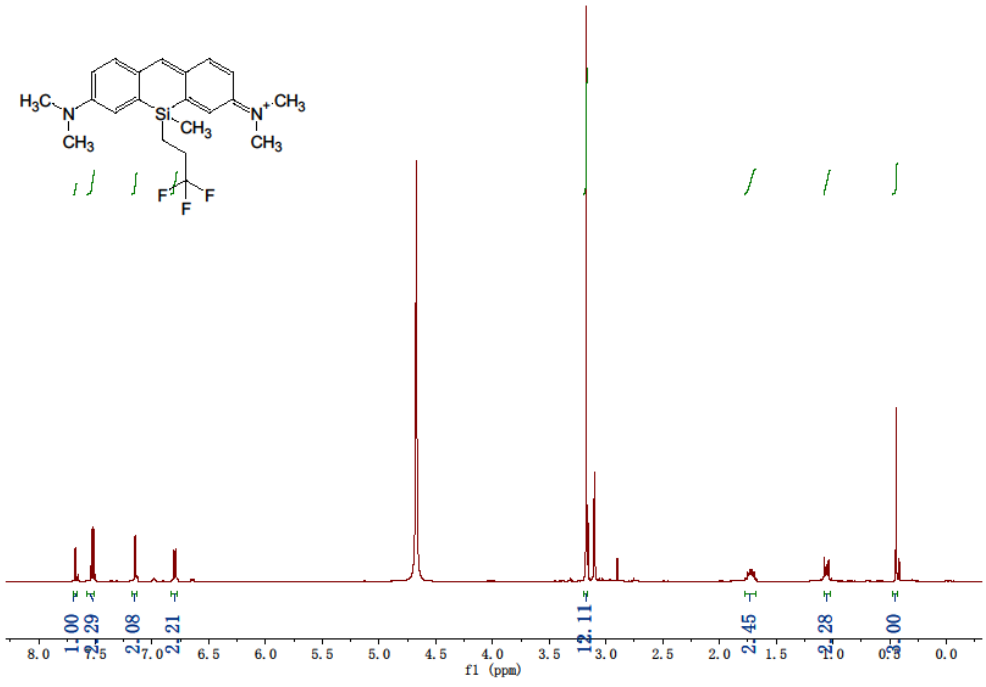

Figure S21. ^{1}H-NMR of SiP-F

No.	Formula	Ion Formula	Measured m/z	Calc m/z	ppm
SiP-F	C21 H26 F3 N2 Si	C21 H26 F3 N2 Si	391.1815	391.1812	-0.77

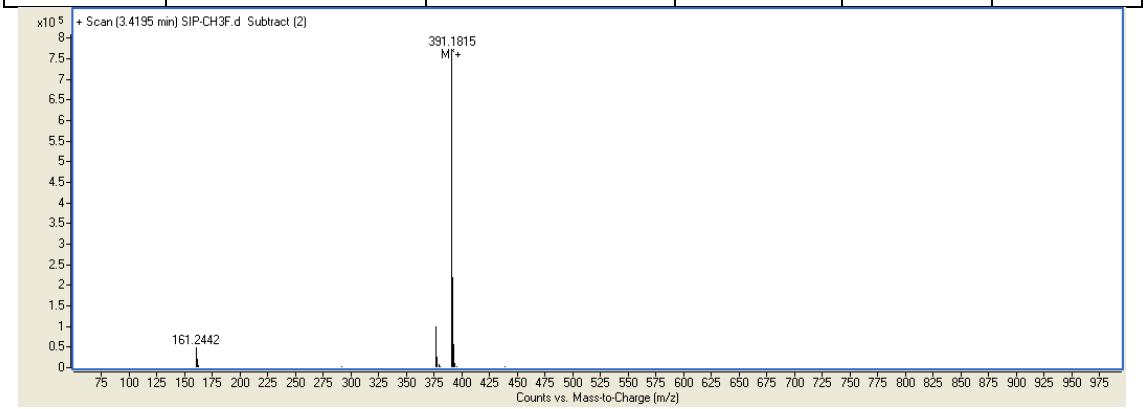

Figure S22. HRMS of SiP-F

Characterization of SiP-Pr

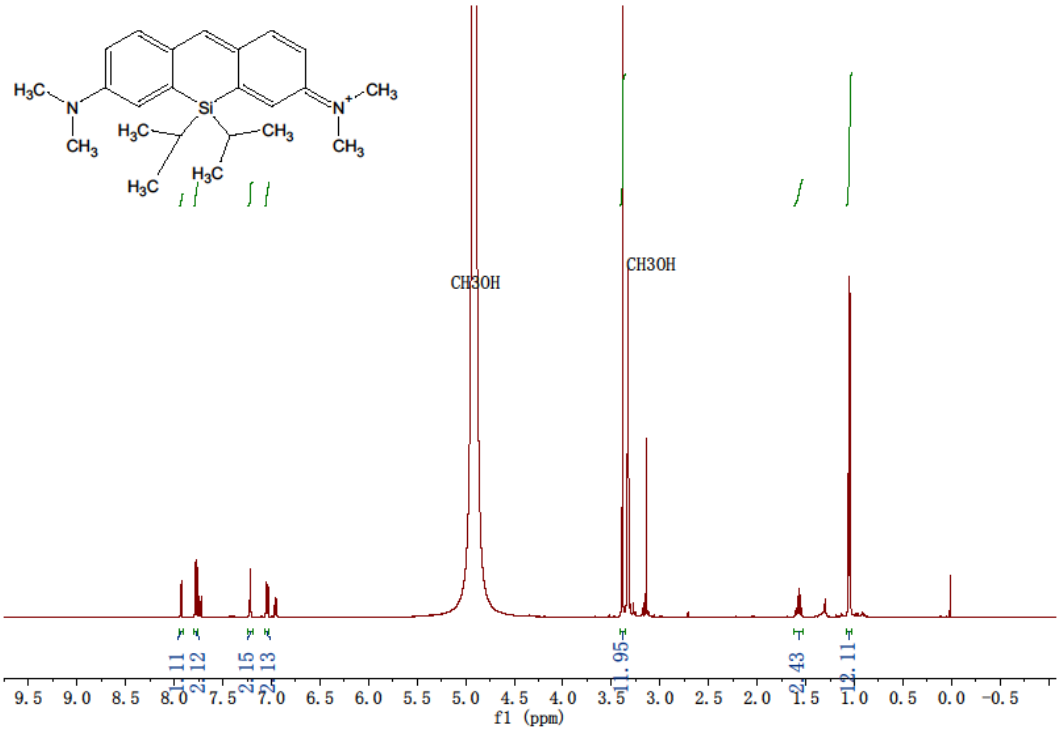

Figure S23. ^{1}H-NMR of SiP-Pr

Sample	Formula	Ion Formula	Measured m/z	Calc m/z	ppm
SiP-Pr	C23 H33 N2 Si	C23 H33 N2 Si	365.2411	365.2408	-0.79

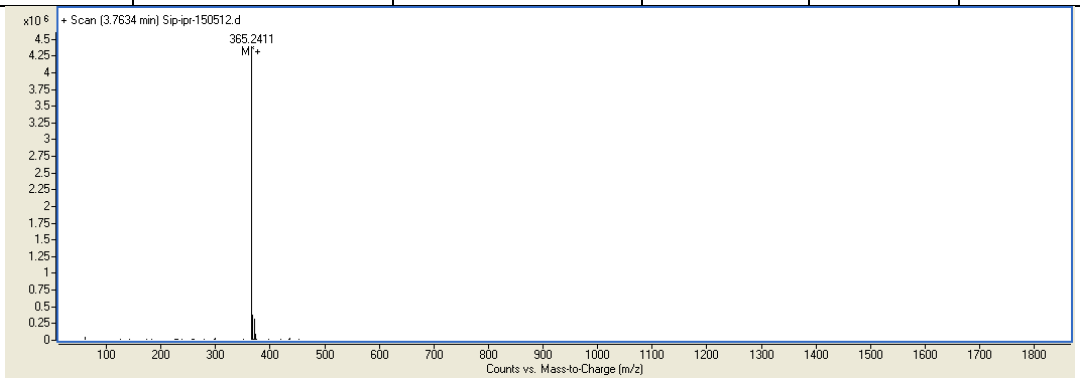

Figure S24. HRMS of SiP-Pr

Characterization of SiP-Ph

No.	Formula	Ion Formula	Measured m/z	Calc m/z	ppm
SiP-Ph	C29 H29 N2 Si	C29 H29 N2 Si	433.2095	433.2095	0

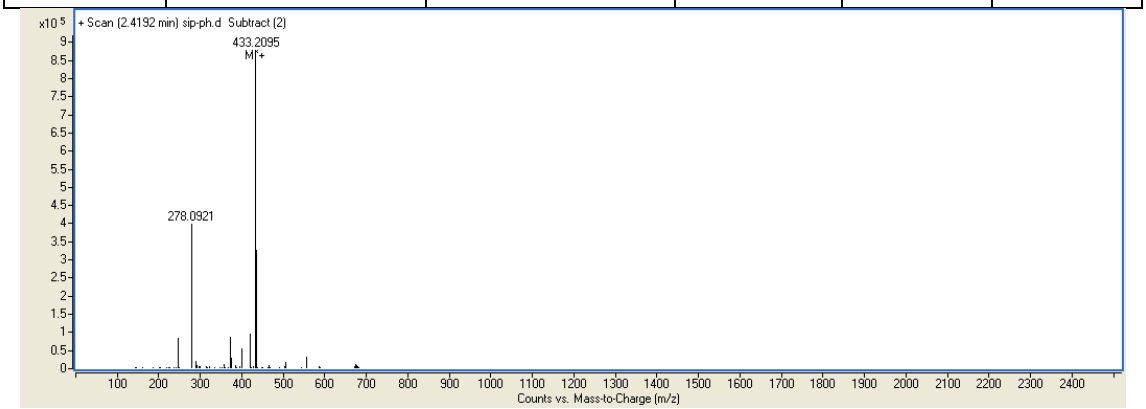

Figure S25. HRMS of SiP-Ph